Applications of Spherical Harmonics
to Analysis of Spherical Data

Friday Feature™, M. Gold

physics 492, Spring 2017

http://spud.spa.umn.edu/~pryke/logbook/20000922/

multipole components up to l=3. The color scale is ±0.9 common across all the plots.

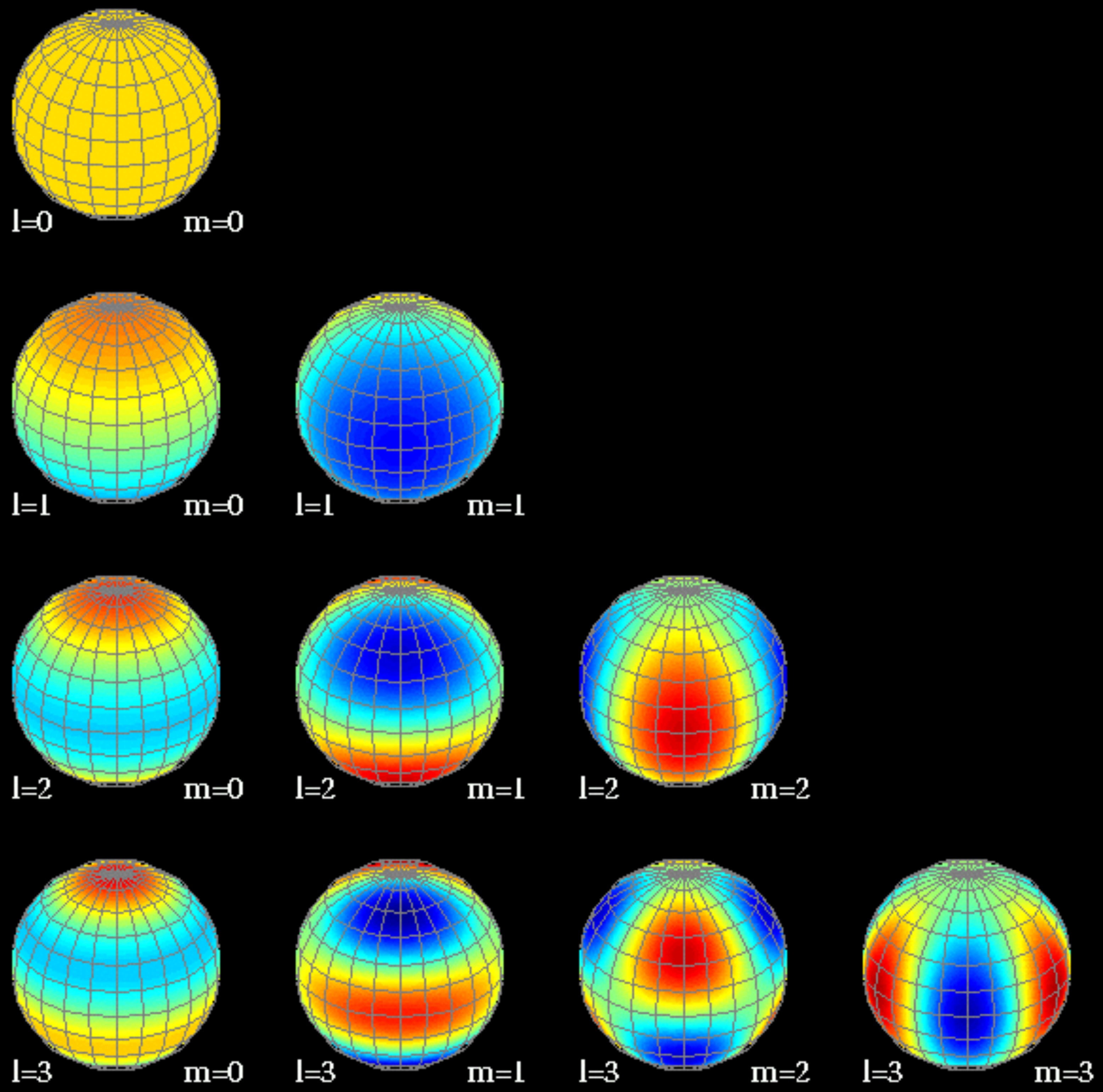

The Gravity Recovery and Climate Experiment (GRACE)

Mission is designed to monitor local, regional, and global changes in the Earth's gravity field. The changes observed in the gravity field are a manifestation of mass being transported in the Earth's oceans, atmosphere, and on land surfaces. Analysis of the data delivered by GRACE yields a direct measure of mass flux with high spatial resolution on the Earth's surface.

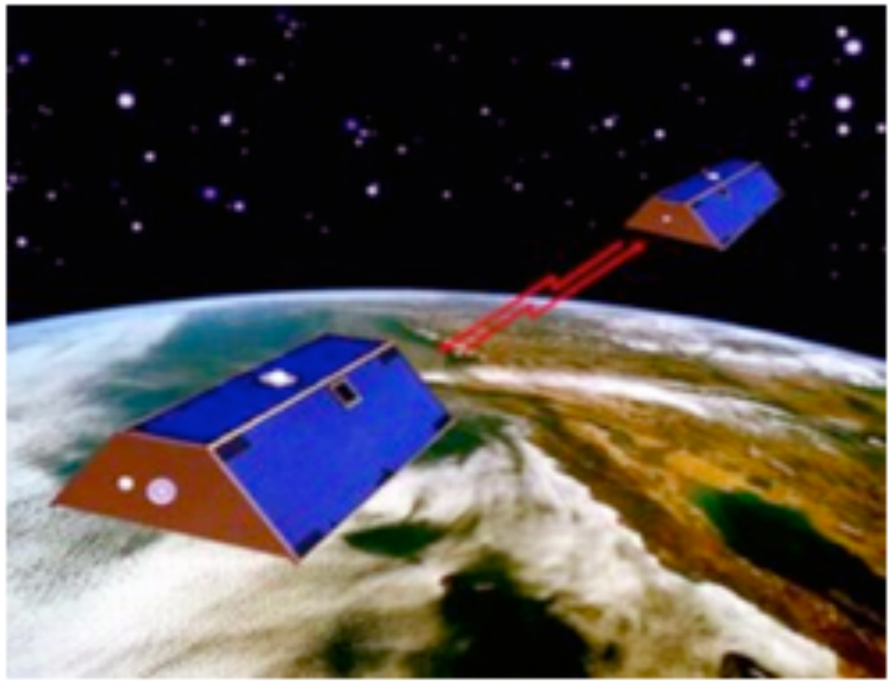

Figure 1

Nevertheless, spherical harmonic models of the gravity field produced to date from GRACE are at least a two orders of magnitude improvement over any former modeling effort (e.g. Lemoine et al. [1998]). This is a result of the special design of the GRACE Mission and its exquisitely accurate measurement of the range-rate between two co-orbiting satellites separated by approximately 250 km using a highly stable K-Band link (KBRR) [Figure 1]. The intersatellite line-of-sight measurement precision delivered by GRACE is well below 1 micron/sec. This gives GRACE unique sensitivity to the accelerations induced on low Earth orbiting satellites from the surface mass along the satellite's ground track.

The first 111 days of preliminary data from GRACE were used to produce a map of the Earth's gravity anomalies. A gravity anomaly map shows us how much the actual Earth's gravity field departs from "normal" as defined by a simplified mathematical gravity model that assumes the Earth is perfectly smooth and featureless. In this grayscale representation, brighter areas represent positive gravity anomalies (note the Andes mountain range in South America), while darker areas represent negative gravity anomalies (note the Puerto Rico trench and the area around Hudson Bay in Canada.) The gravity anomalies (measured in milligals—a unit of gravity acceleration named after Galileo) are only about one-millionth as strong as the actual gravity field, yet GRACE is sensitive enough to produce a detailed map of the variations like this one. Even more accurate maps will follow as the GRACE mission progresses. It is expected that GRACE will eventually be able to detect anomalies approaching one-billionth the strength of the Earth's average gravity field.

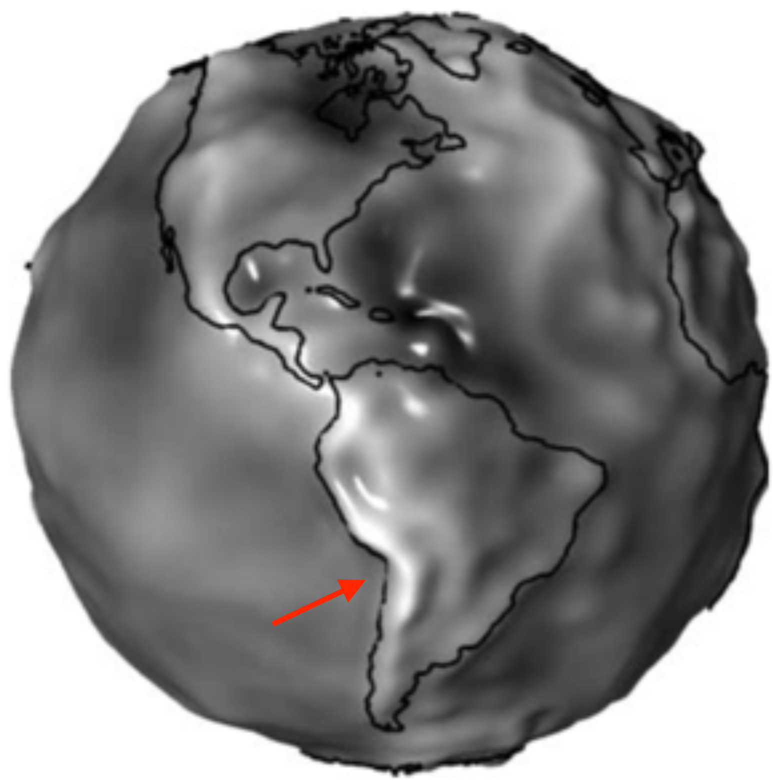

Earth's Gravity Field Anomalies (milligals)

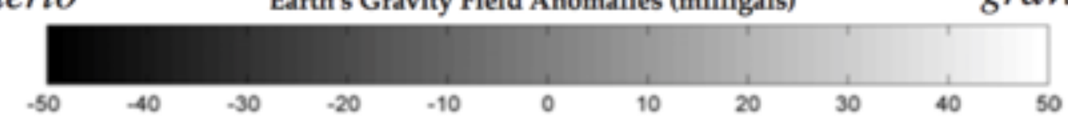

also, see 2014

https://academic.oup.com/gji/article-lookup/doi/10.1093/gji/ggu402

Solution “noise” after “signal” removed

LMAX=20

Residual RMS height H2O, over July 2003 to July 2004 gravity solutions (to degree and order 20), after a trend, annual and semi-annual signal has been removed.

30 stripes - order 15/16

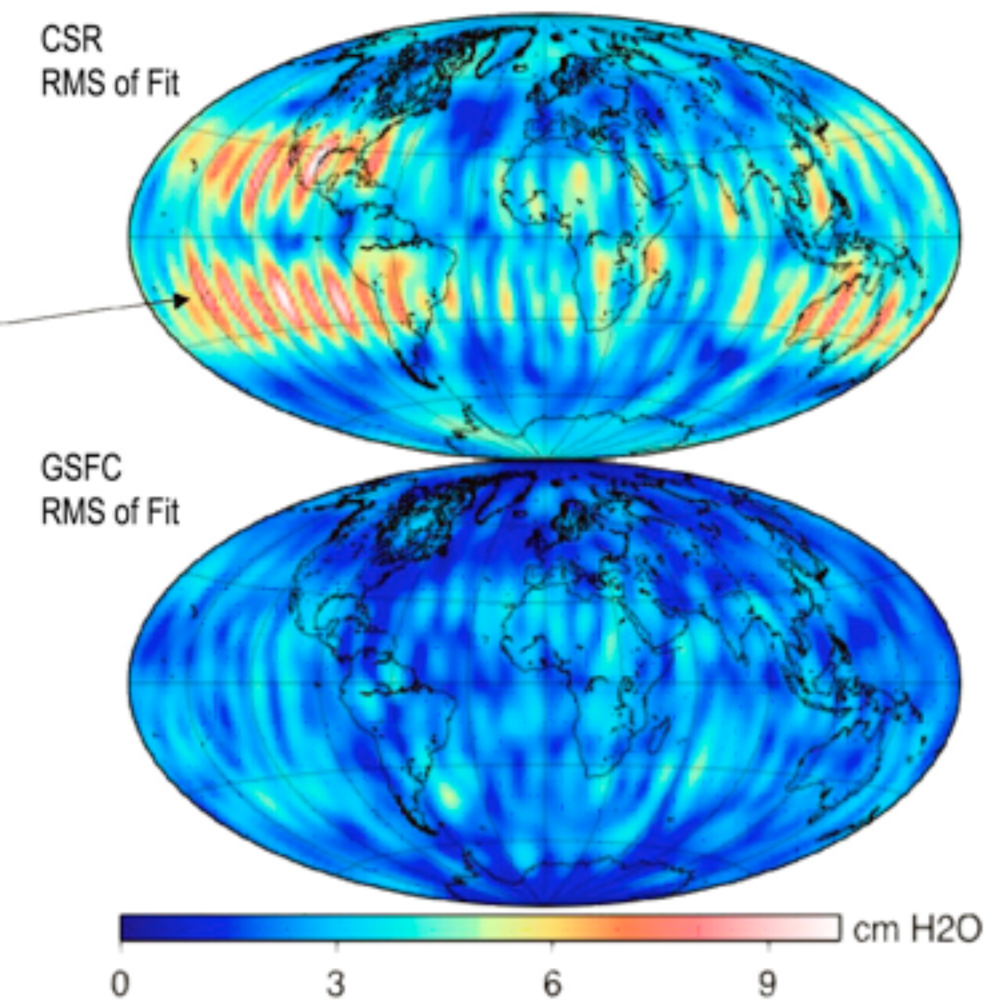

CSR

RMS = 3.7 cm

Max. = 12.0 cm

GSFC

RMS = 2.2 cm

Max. = 5.6 cm

Luthcke et al. 2005, NASA GSFC, Code 697

Figure 2 *A comparison of aliasing in the GSFC and CSR monthly gravity fields after removal of the dominant geophysical signals -- a linear trend, annual and semi-annual term for each harmonic as compared to the mean annual field.*

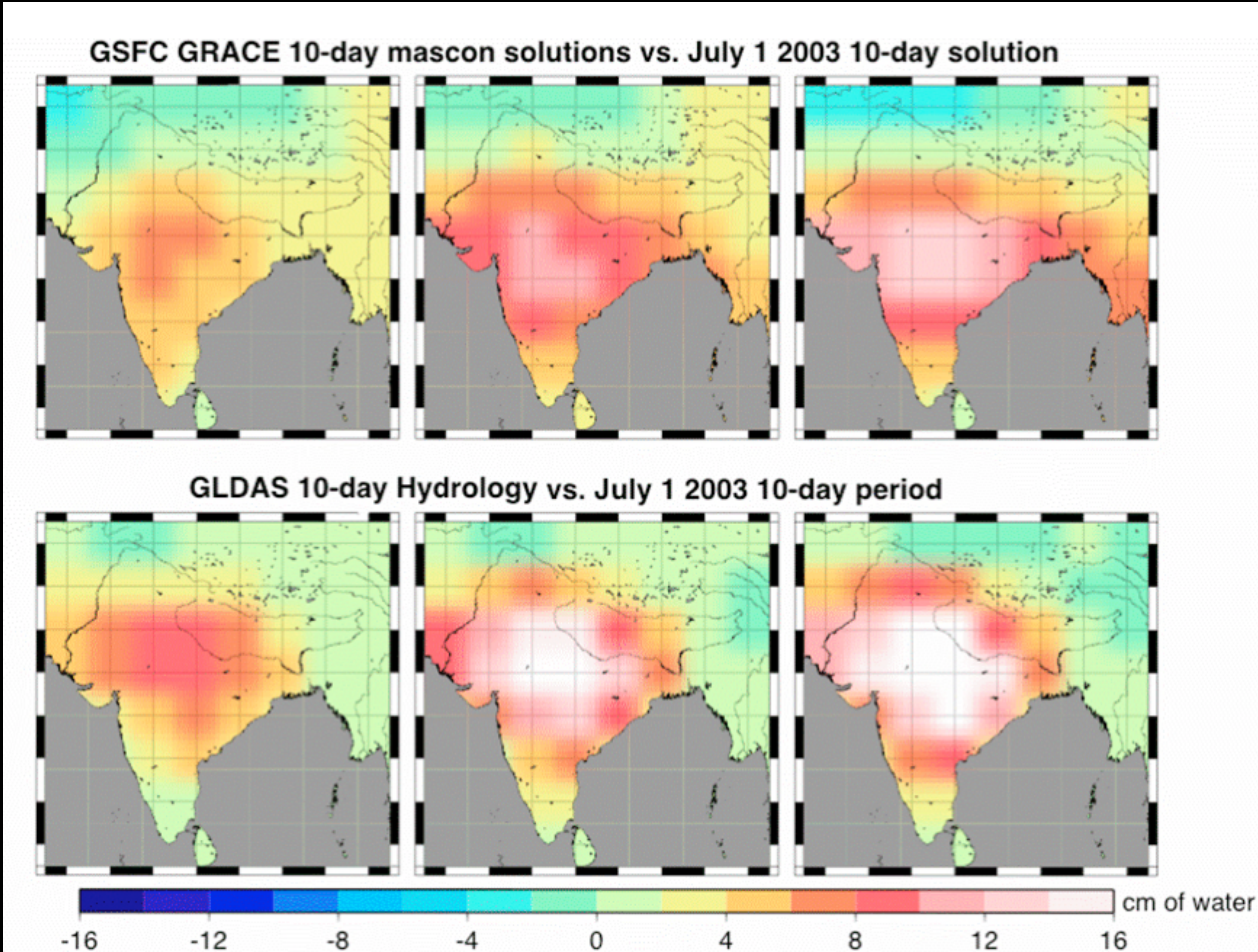
GSFC GRACE 10-day mascon solutions vs. July 1 2003 10-day solution
GLDAS 10-day Hydrology vs. July 1 2003 10-day period
cm of water
-16
-12
-8
-4
0
4
8
12
16

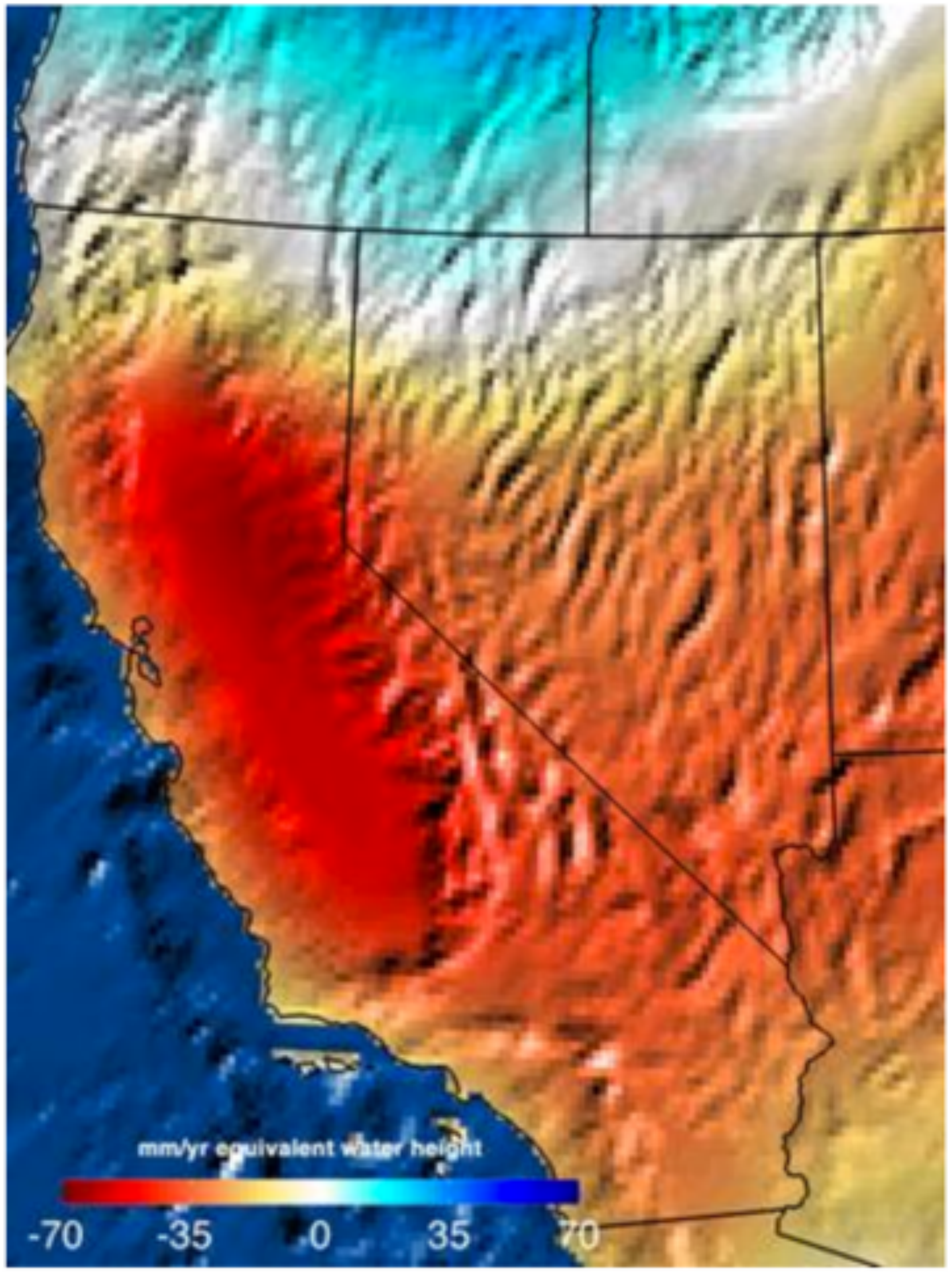

NASA GRACE satellite data reveal the severity of California's drought on water resources across the state. This map shows the trend in water storage between September 2011 and September 2014.

Credits: NASA JPL

GRACE animation

It will take about 11 trillion gallons of water (42 cubic kilometers) -- around 1.5 times the maximum volume of the largest U.S. reservoir -- to recover from California's continuing drought.

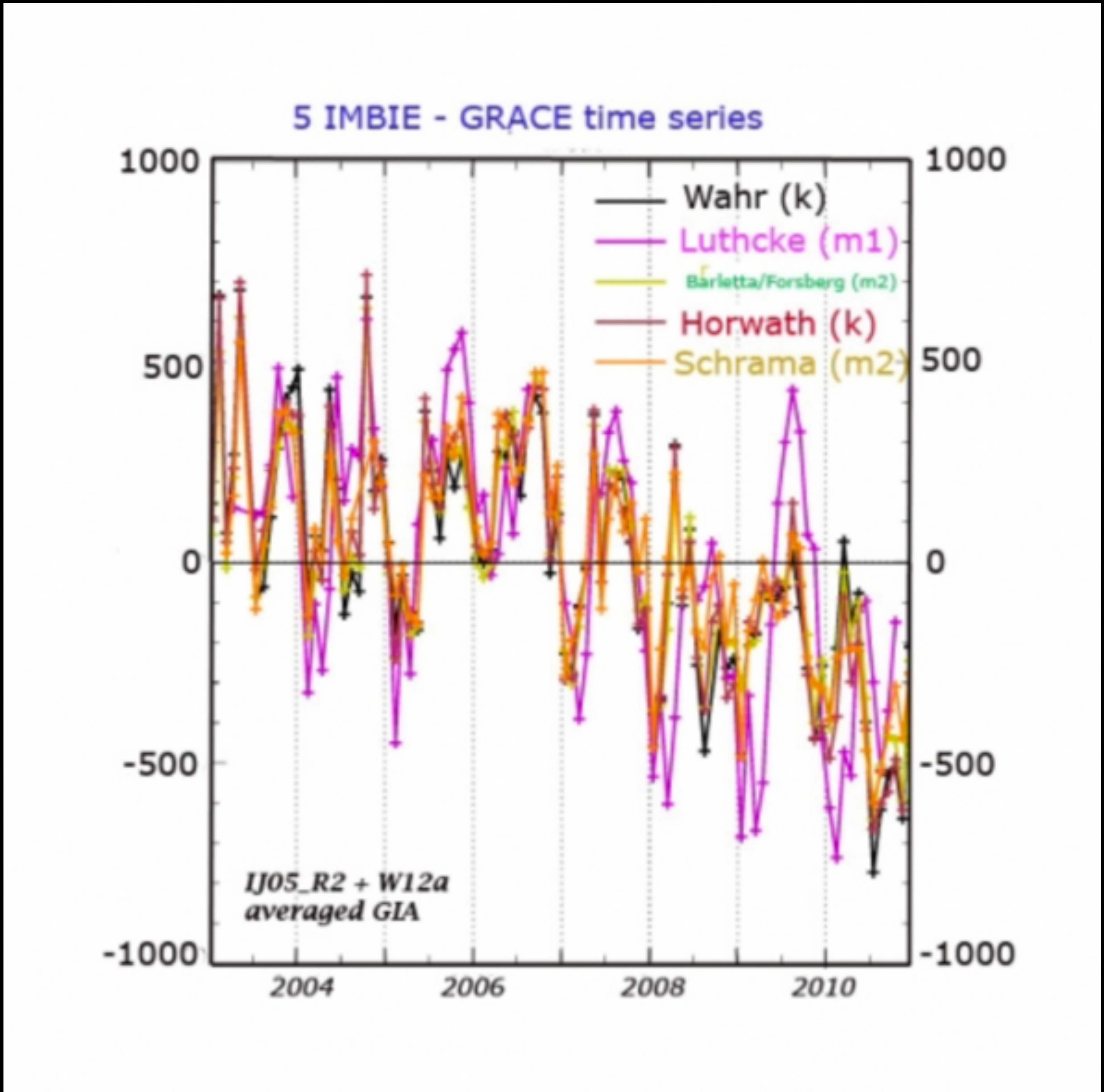

Monthly changes in Antarctic ice mass (gigatons)

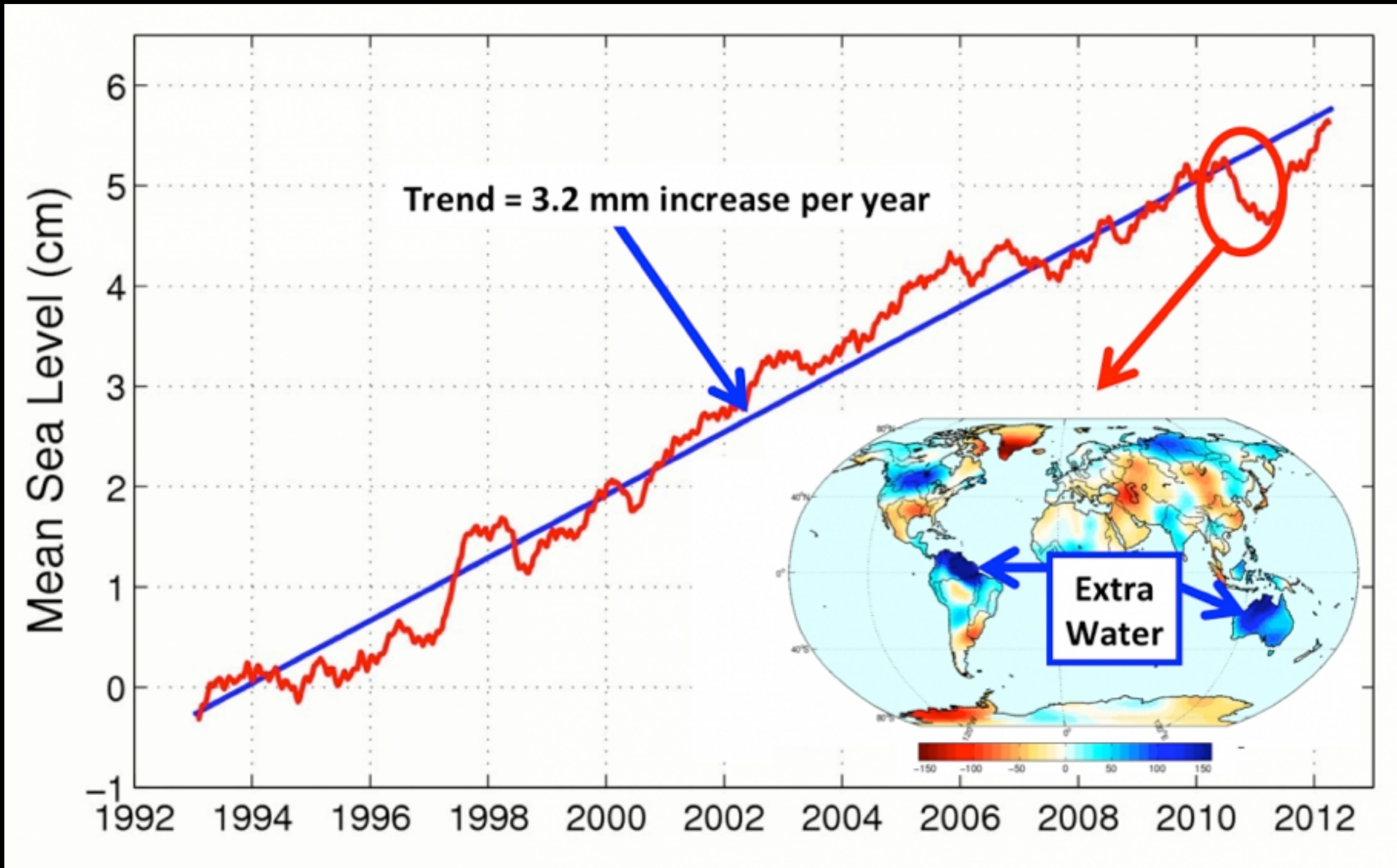

This figure shows changes in global mean sea level …between 1992 to 2012. The data have been averaged to account for long time scale ...

Global Heat Flow with Spherical Harmonic Smoothing

http://www.earth.lsa.umich.edu/~shaopeng/IHFC/heatflow.html

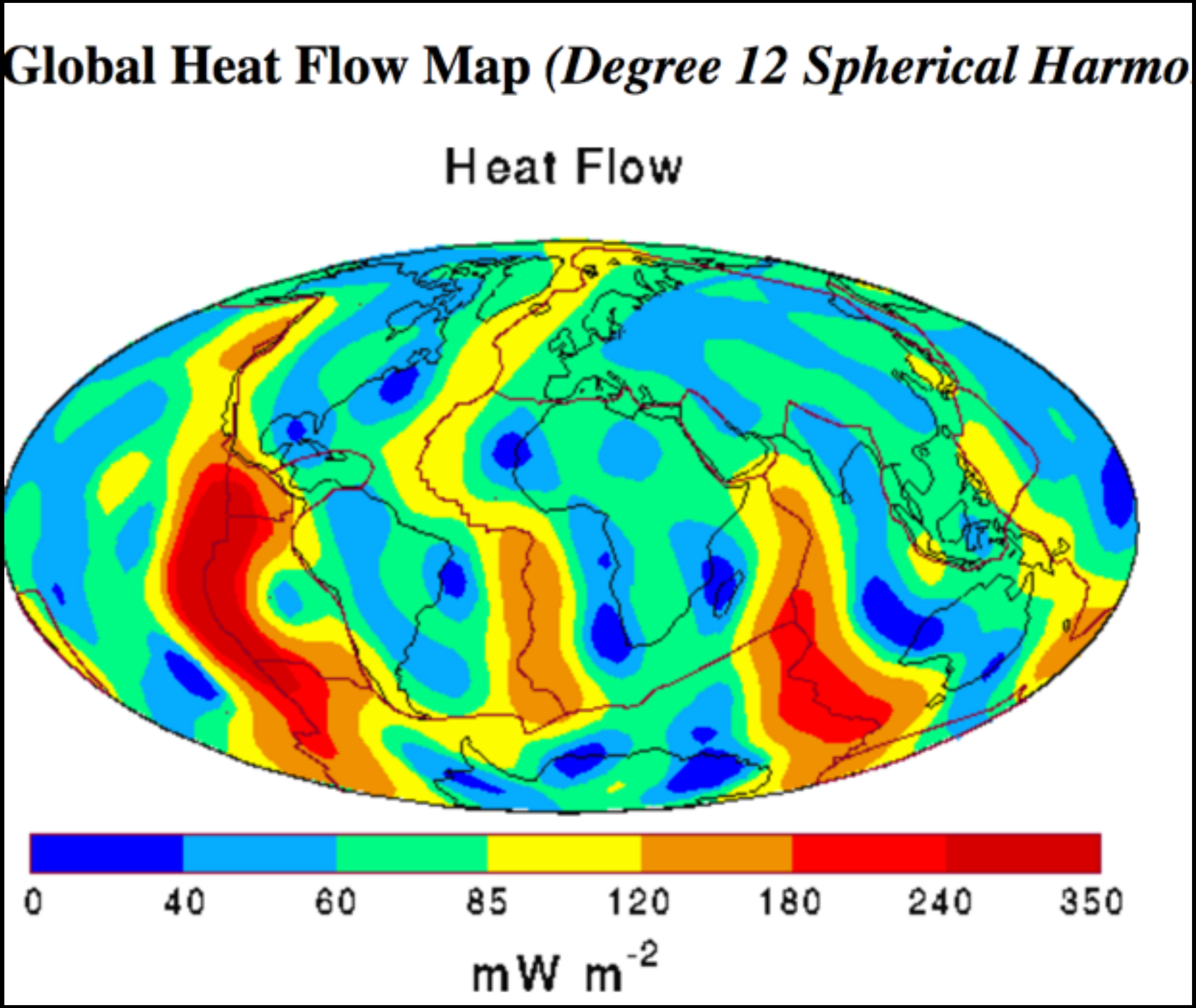

This map shows color-coded contours of the global distribution of heat flow at the surface of the Earth's crust.

HIPPOCAMPAL SURFACE ANALYSIS USING SPHERICAL HARMONIC FUNCTION APPLIED TO SURFACE CONFORMAL MAPPING

Boris Gutman[1], *Yalin Wang*[1,2], *Lok Ming Lui*[1], *Tony F. Chan*[1], *Paul M. Thompson*[2]

[1] Department of Mathematics, University of California, Los Angeles, CA USA
[2] Department of Neurology, UCLA Medical School, Los Angeles, CA USA
ylwang@math.ucla.edu

ABSTRACT

Using spherical harmonics of an inverse conformal map, we compared hippocampal surfaces of sixteen Alzheimer (AD) and fourteen control subjects. Hippocampal surfaces were conformally mapped to a sphere. Maps were regularly sampled and exact, high-degree spherical harmonic transforms of the inverse maps were computed. Using the transforms shape descriptors corresponding to the degree of the harmonics and invariant to translation, rotation, and scale were obtained and normalized against sample mean. Two-dimensional visualizations of the shape descriptors were indicative of global as well as local shape features of hippocampal surfaces. These descriptors are potentially useful for visual detection of global patterns and creation of population-based, probabilistic, disease-specific digital atlases, especially for comparison of global shape features.

[1] have employed this method in their study of Alzheimer's.

Fig. 1. Low-Pass Filtering: (a) through (d) are hippocampal surfaces reconstructed from harmonics up to degree 10, 20, 63 and 127, respectively. (e) is the original hippocampus

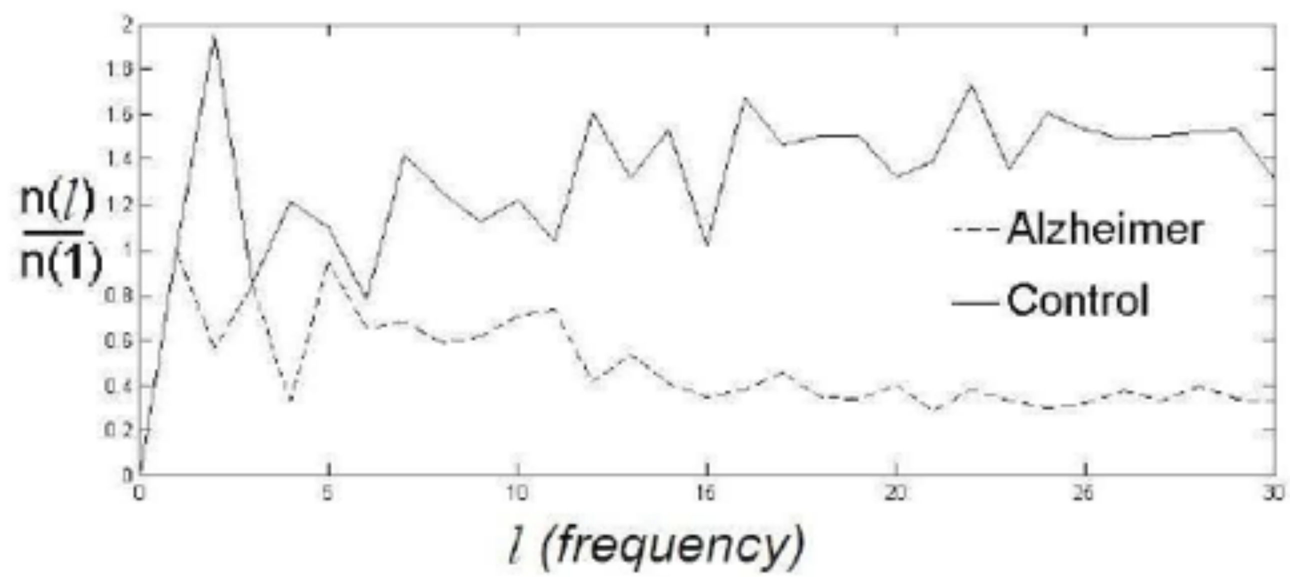

Fig. 3. Plots of normalized descriptors for two hippocampi: higher relative magnitude in lower frequency descriptors of the solid line indicates a greater presence of low-frequency curves in the control hippocampus.

https://arxiv.org/pdf/1612.00338v2.pdf

Hippocampus Temporal Lobe Epilepsy Detection Using a Combination of Shape-based Features and Spherical Harmonics Representation

Dec 2916

Zohreh Kohan ·
Hamidreza Farhidzadeh ·
Reza Azmi ·

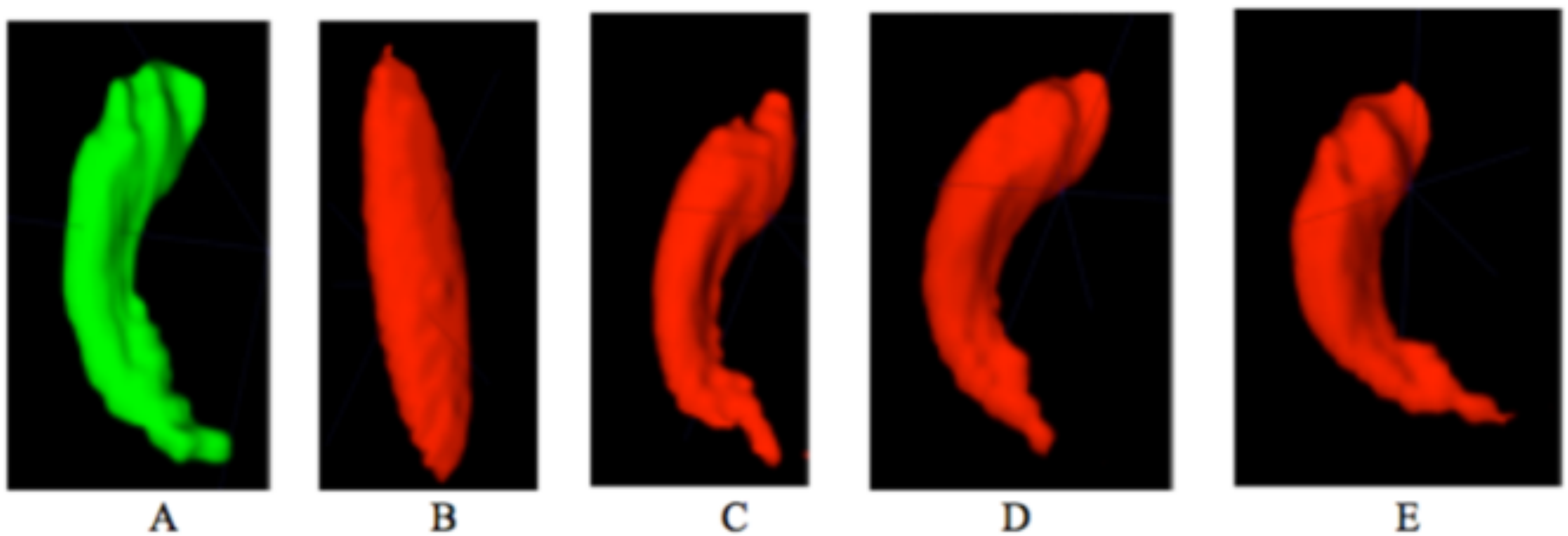

Fig. 3 A) 3D shape of left hippocampus and (B-E) its reconstruction through SPHARM based shape reconstruction using (B) $L-max$=1 (C) $L-max$ =8 (D) $L-max$ =16 and (E) $L-max$ =24

"…could be helpful to describe the hippocampus shape deformation and could be used in diagnosis of the temporal lobe epilepsy disease in MRI."

Cosmic Microwave Background (CMB)

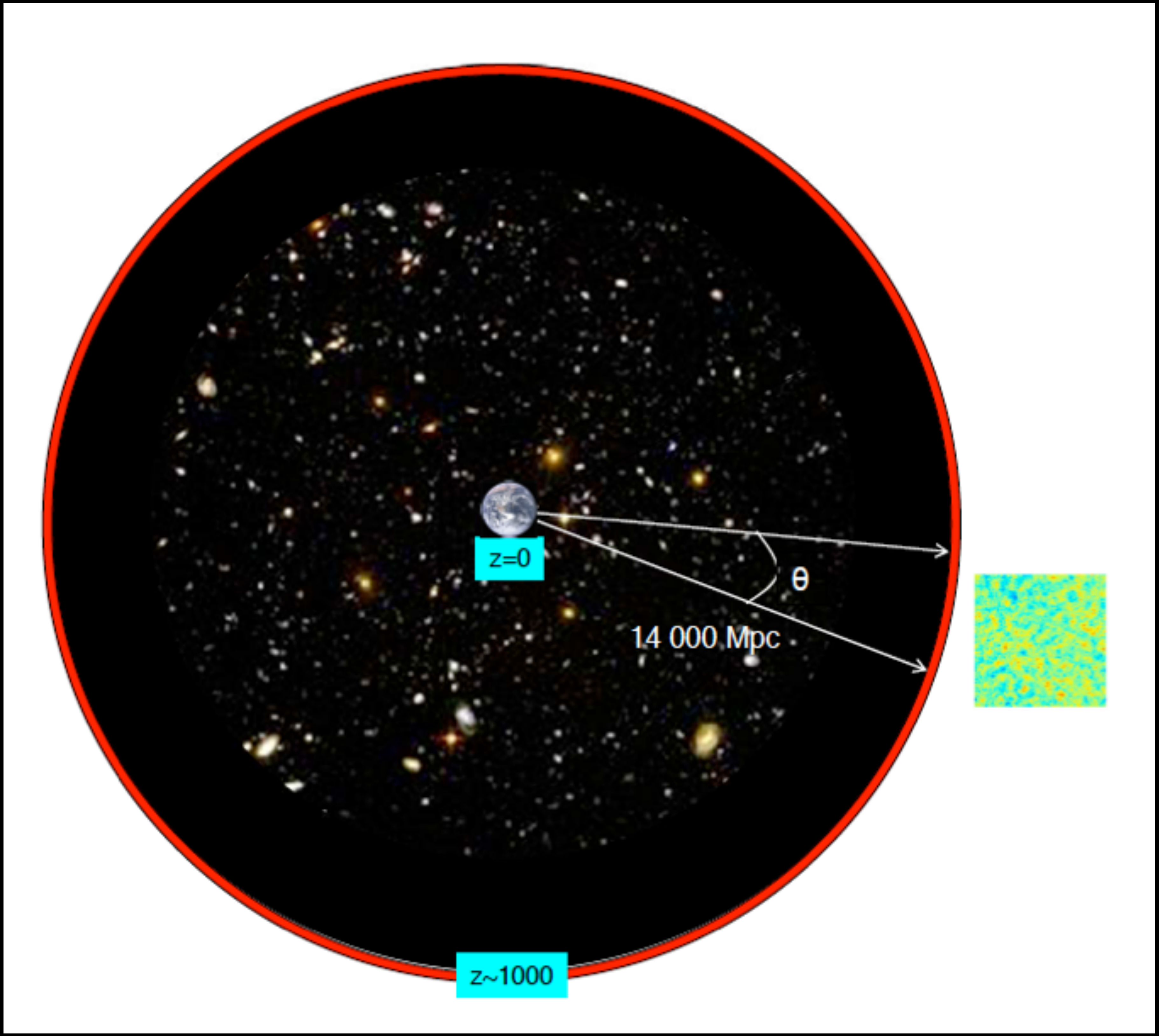

Planck explorer satellite 2009-2013

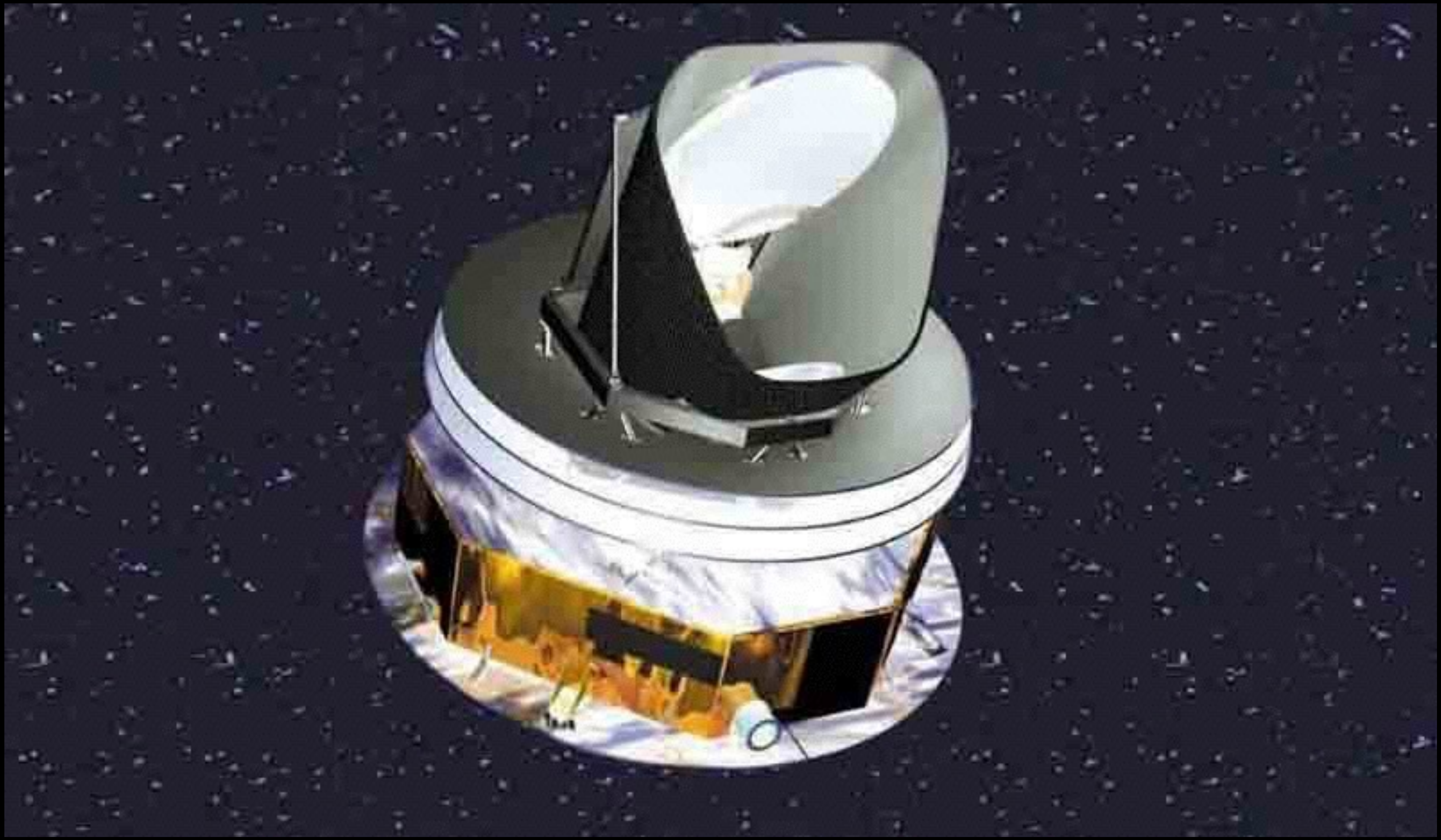

Friday Feature™, M. Gold   physics 492, Spring 2017

Cosmological red shift (z)

$$1 + z = \lambda_{obs}/\lambda_{emit} = a_{now}/a_{then}$$

where "a" is expansion factor

age of universe:
13.799±0.021 Gy
ΛCDM concordance model.

Red line is our universe in which expansion is accelerating

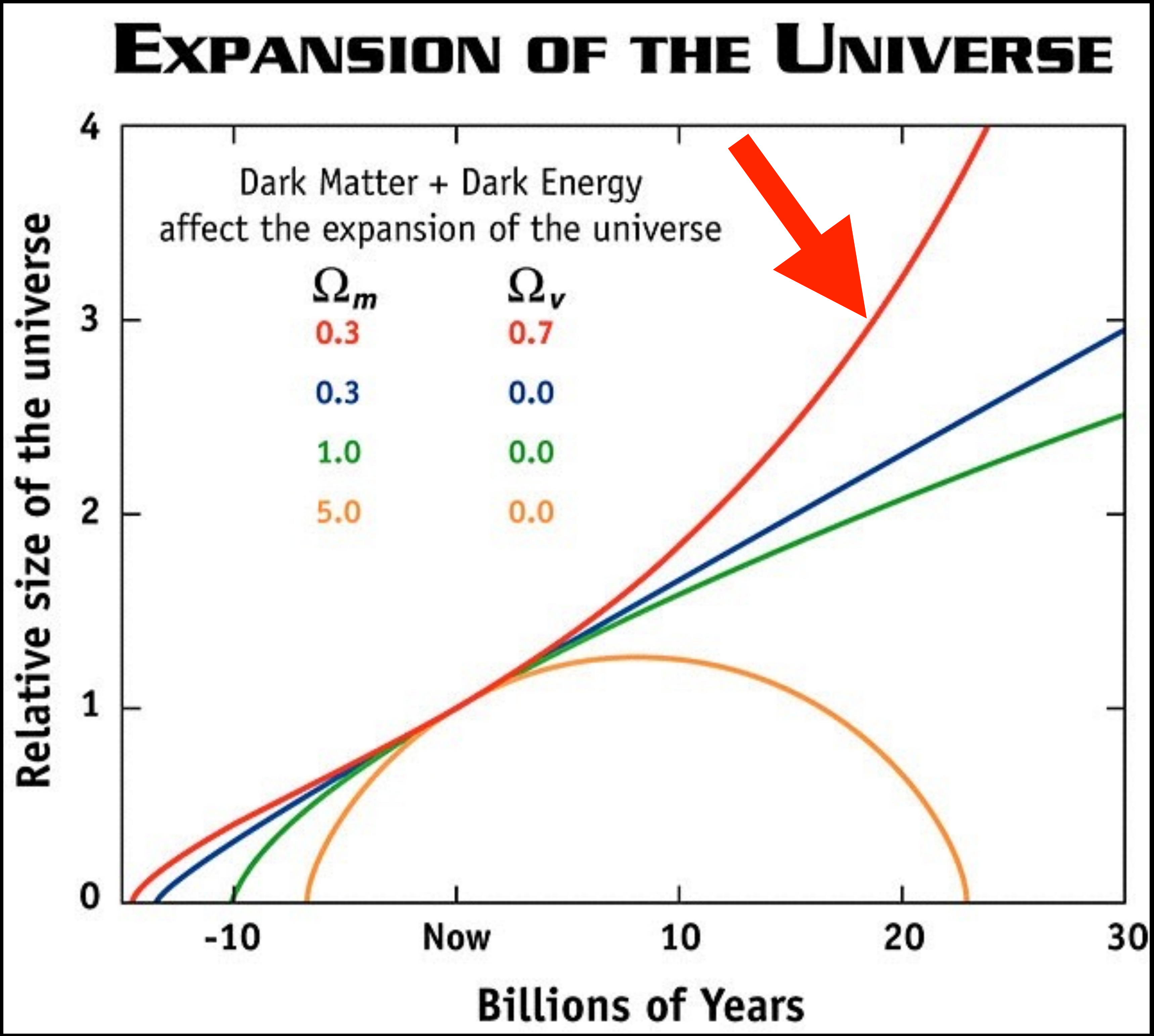

Perfect Black Body T=2.725 K

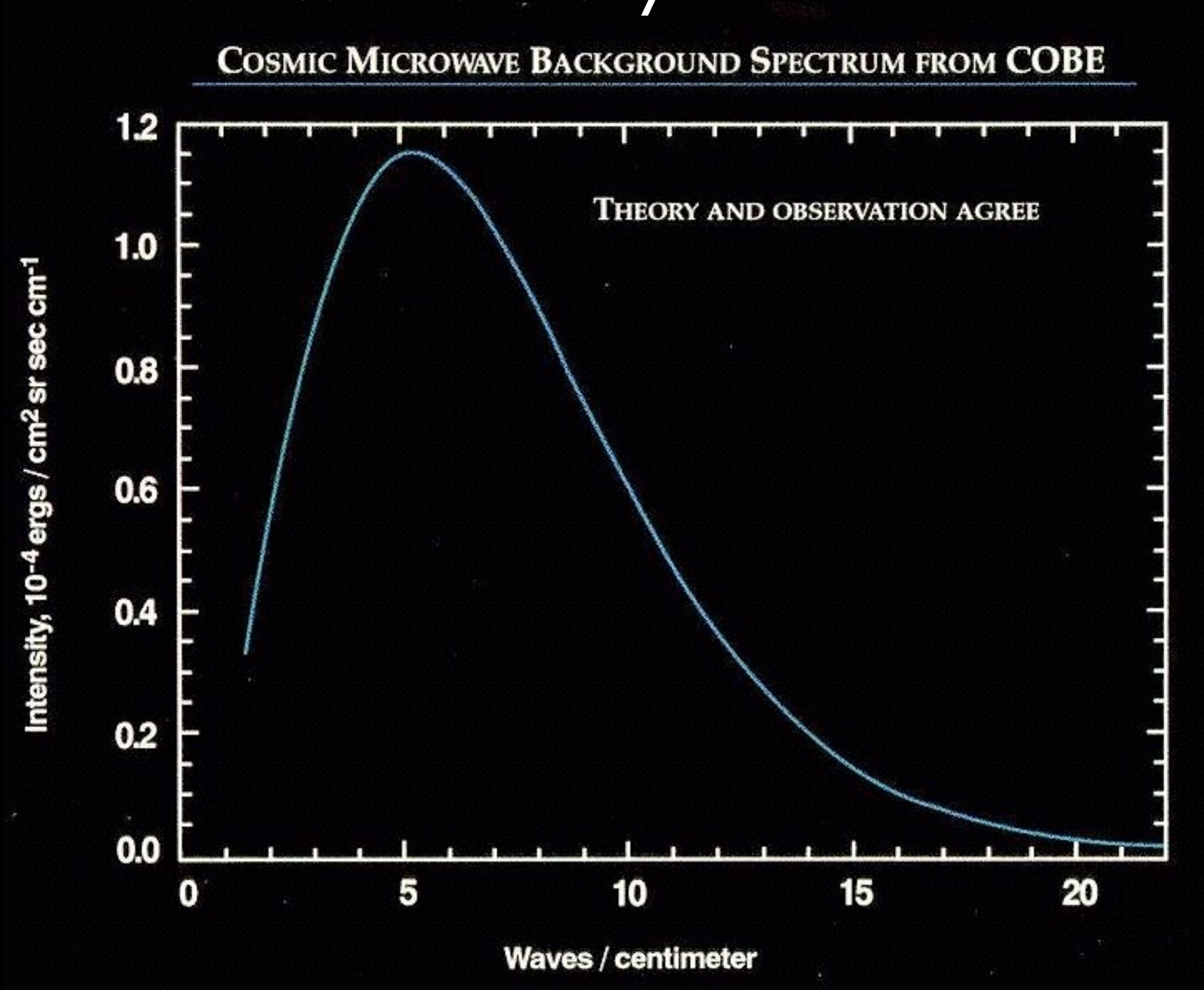

Dipole Moment $\ell = 1$

V = 600 km/s in direction of Virgo Cluser

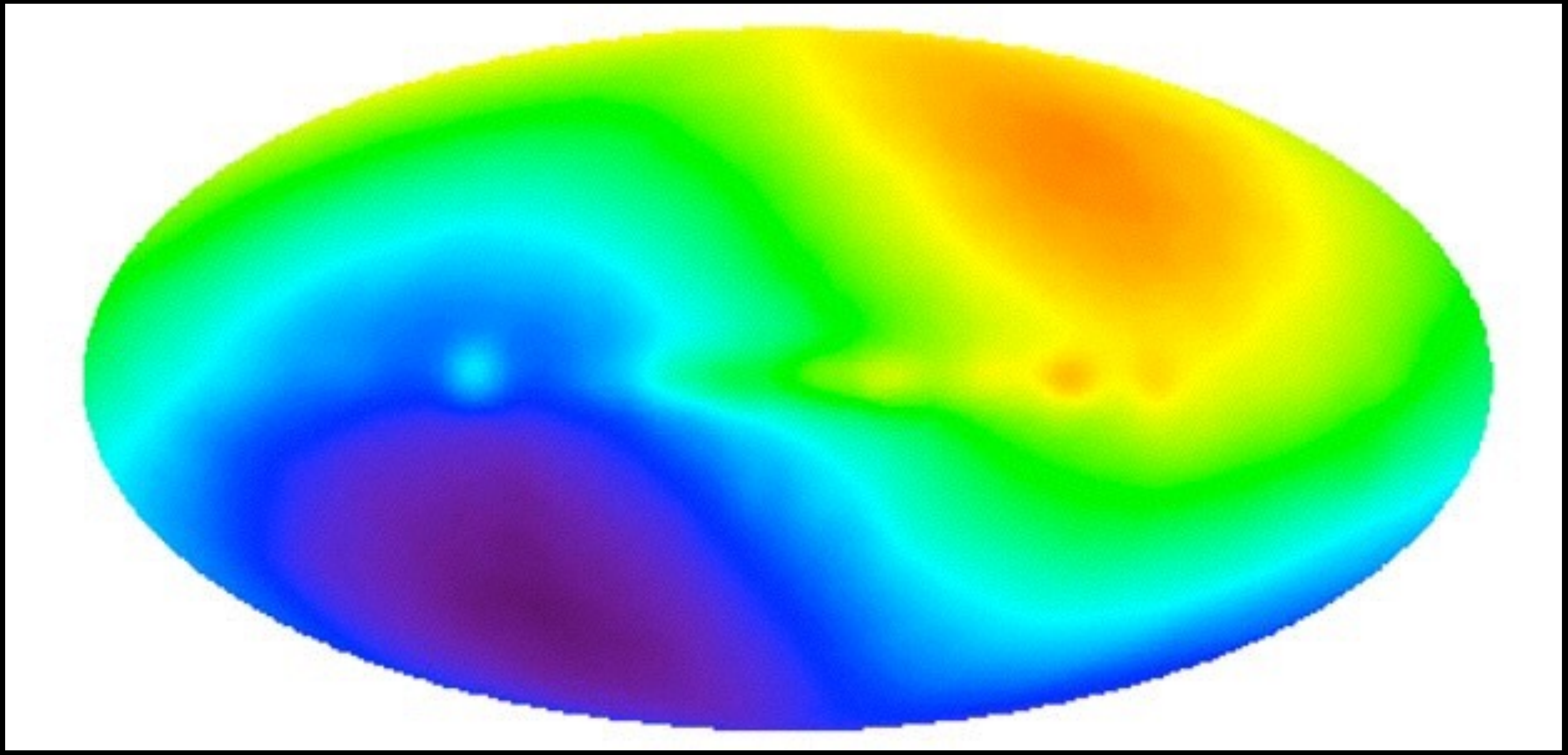

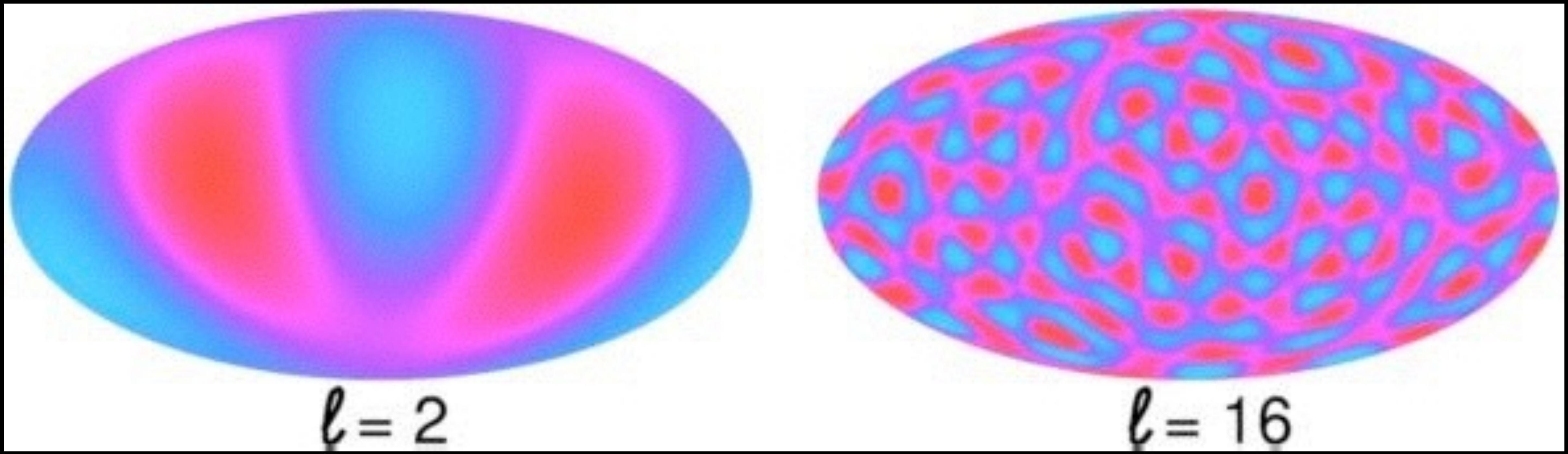
ℓ = 2
ℓ = 16

Temperature Fluctuations $\Delta T/T \sim 10^{-5}$

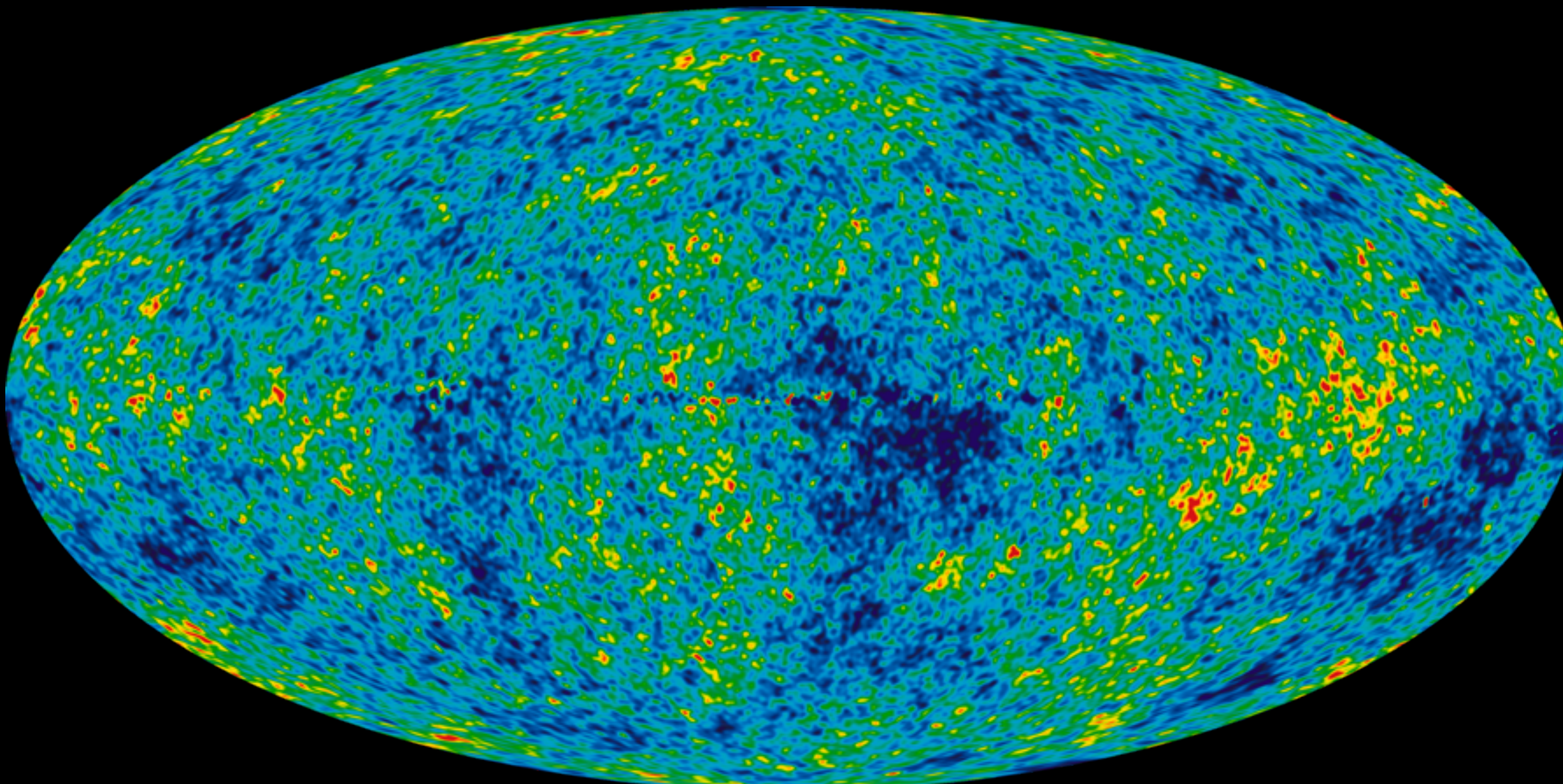

auto correlation function:

$$w(\theta_{12}) = \langle \frac{\Delta T}{T}(\theta_1) \frac{\Delta T}{T}(\theta_2) \rangle$$

Expand in Spherical Harmonics, use spherical symmetry (no m dependence) and obtain multipole coefficients

$$\frac{\ell(\ell+1)}{2\pi} C_\ell^2 \ [\mu K^2]$$

primordial pressure (acoustic) oscillations

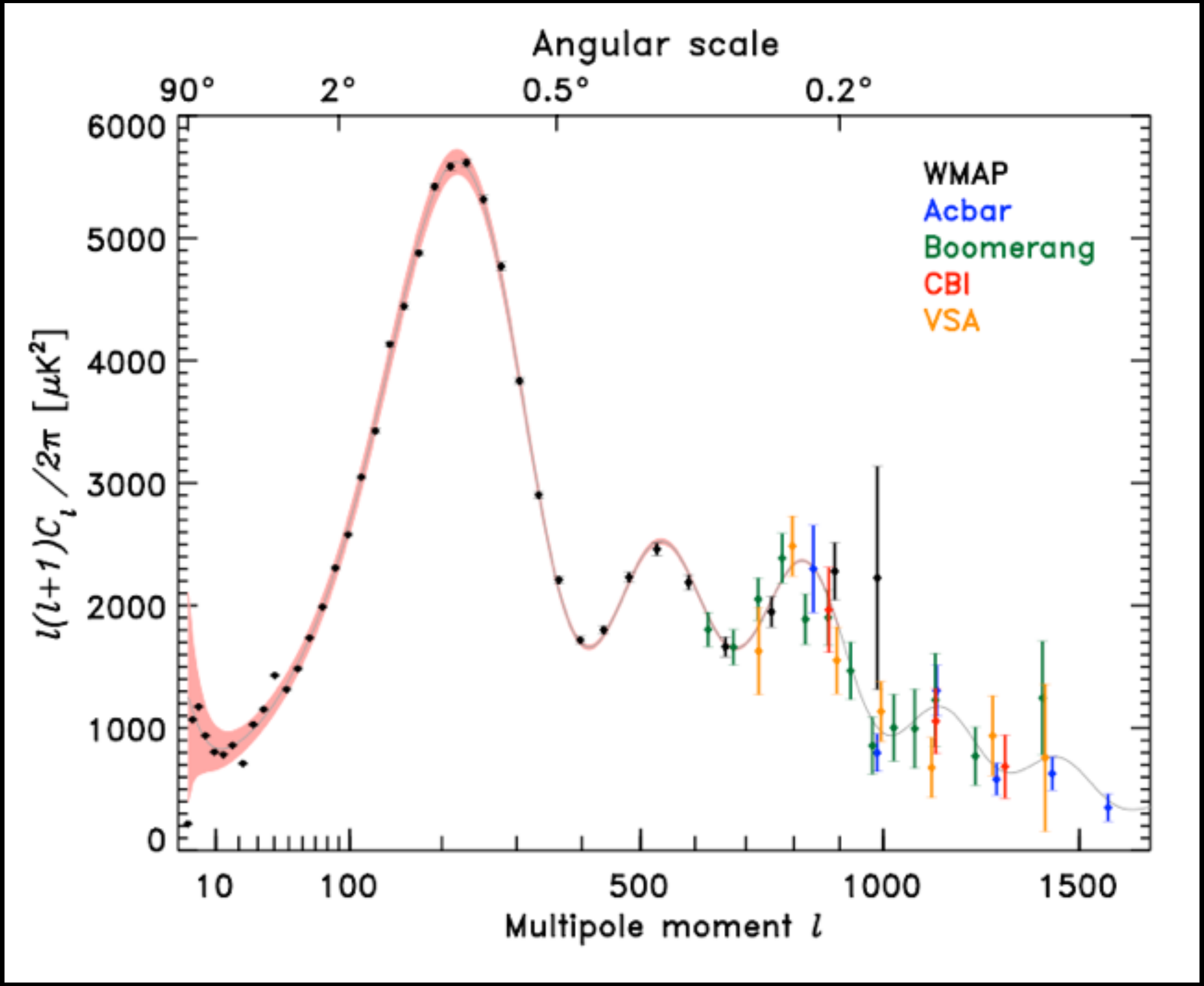

$$\ell \sim 100^\circ/\theta$$

Measered cosmological parameters: the densities of baryonic matter, dark matter and dark energy (Ω_b, Ω_m, Ω_Λ), and the spectral index (n_s), which describes the relative amount of primordial fluctuations (seeds of nascent cosmic structures)

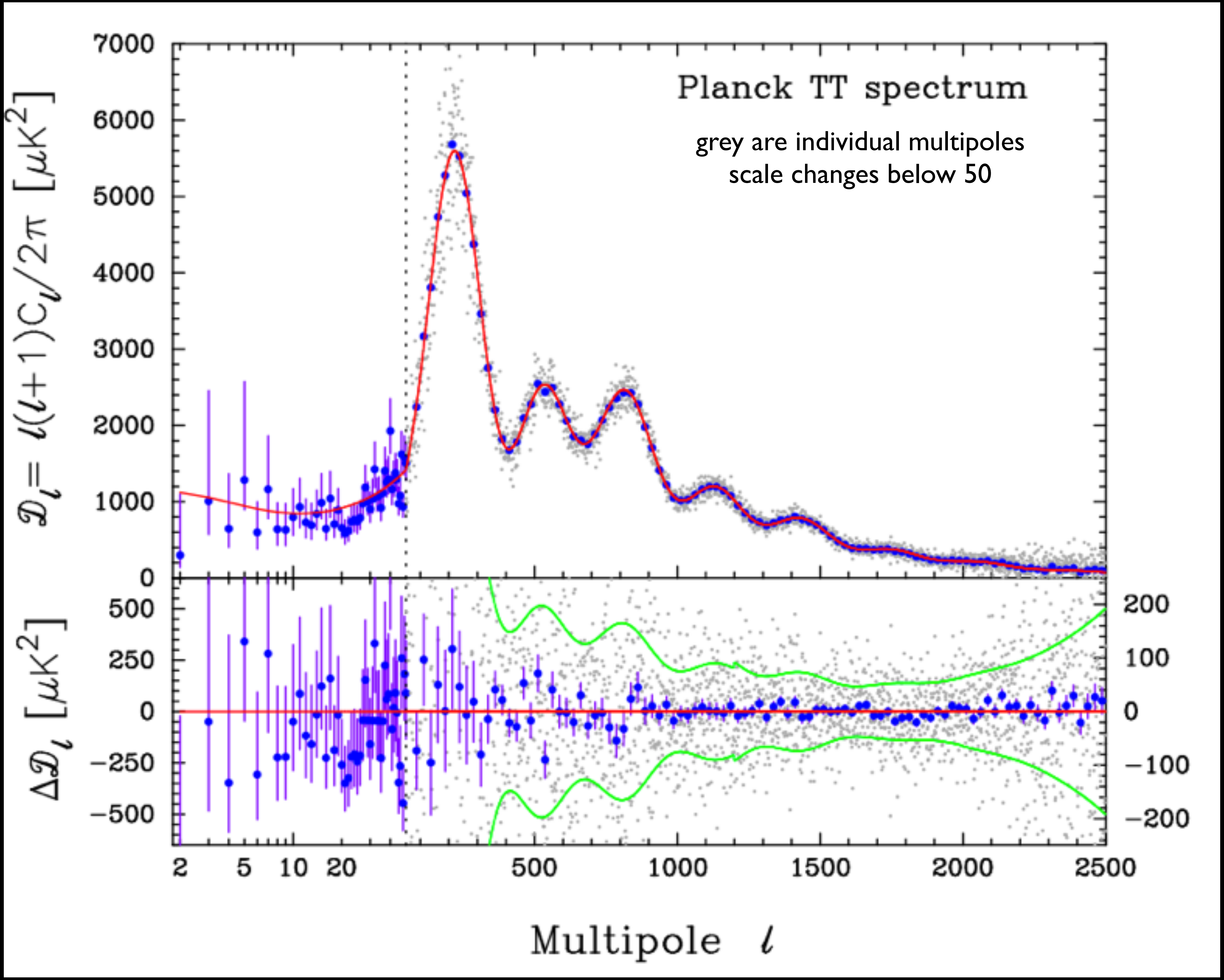

http://planck.caltech.edu/pub/2013results/Planck_2013_results_16.pdf

Planck Collaboration: Cosmological parameters

	Planck		*Planck*+lensing		*Planck*+WP	
Parameter	Best fit	68% limits	Best fit	68% limits	Best fit	68% limits
$\Omega_b h^2$	0.022068	0.02207 ± 0.00033	0.022242	0.02217 ± 0.00033	0.022032	0.02205 ± 0.00028
$\Omega_c h^2$	0.12029	0.1196 ± 0.0031	0.11805	0.1186 ± 0.0031	0.12038	0.1199 ± 0.0027
$100\theta_{MC}$	1.04122	1.04132 ± 0.00068	1.04150	1.04141 ± 0.00067	1.04119	1.04131 ± 0.00063
τ	0.0925	0.097 ± 0.038	0.0949	0.089 ± 0.032	0.0925	$0.089^{+0.012}_{-0.014}$
n_s	0.9624	0.9616 ± 0.0094	0.9675	0.9635 ± 0.0094	0.9619	0.9603 ± 0.0073
$\ln(10^{10} A_s)$	3.098	3.103 ± 0.072	3.098	3.085 ± 0.057	3.0980	$3.089^{+0.024}_{-0.027}$
Ω_Λ	0.6825	0.686 ± 0.020	0.6964	0.693 ± 0.019	0.6817	$0.685^{+0.018}_{-0.016}$
Ω_m	0.3175	0.314 ± 0.020	0.3036	0.307 ± 0.019	0.3183	$0.315^{+0.016}_{-0.018}$
σ_8	0.8344	0.834 ± 0.027	0.8285	0.823 ± 0.018	0.8347	0.829 ± 0.012
z_{re}	11.35	$11.4^{+4.0}_{-2.8}$	11.45	$10.8^{+3.1}_{-2.5}$	11.37	11.1 ± 1.1
H_0	67.11	67.4 ± 1.4	68.14	67.9 ± 1.5	67.04	67.3 ± 1.2
$10^9 A_s$	2.215	2.23 ± 0.16	2.215	$2.19^{+0.12}_{-0.14}$	2.215	$2.196^{+0.051}_{-0.060}$
$\Omega_m h^2$	0.14300	0.1423 ± 0.0029	0.14094	0.1414 ± 0.0029	0.14305	0.1426 ± 0.0025
$\Omega_m h^3$	0.09597	0.09590 ± 0.00059	0.09603	0.09593 ± 0.00058	0.09591	0.09589 ± 0.00057
Y_P	0.247710	0.24771 ± 0.00014	0.247785	0.24775 ± 0.00014	0.247695	0.24770 ± 0.00012
Age/Gyr	13.819	13.813 ± 0.058	13.784	13.796 ± 0.058	13.8242	13.817 ± 0.048
z_*	1090.43	1090.37 ± 0.65	1090.01	1090.16 ± 0.65	1090.48	1090.43 ± 0.54
r_*	144.58	144.75 ± 0.66	145.02	144.96 ± 0.66	144.58	144.71 ± 0.60
$100\theta_*$	1.04139	1.04148 ± 0.00066	1.04164	1.04156 ± 0.00066	1.04136	1.04147 ± 0.00062
z_{drag}	1059.32	1059.29 ± 0.65	1059.59	1059.43 ± 0.64	1059.25	1059.25 ± 0.58
r_{drag}	147.34	147.53 ± 0.64	147.74	147.70 ± 0.63	147.36	147.49 ± 0.59
k_D	0.14026	0.14007 ± 0.00064	0.13998	0.13996 ± 0.00062	0.14022	0.14009 ± 0.00063
$100\theta_D$	0.161332	0.16137 ± 0.00037	0.161196	0.16129 ± 0.00036	0.161375	0.16140 ± 0.00034
z_{eq}	3402	3386 ± 69	3352	3362 ± 69	3403	3391 ± 60
$100\theta_{eq}$	0.8128	0.816 ± 0.013	0.8224	0.821 ± 0.013	0.8125	0.815 ± 0.011
$r_{drag}/D_V(0.57)$	0.07130	0.0716 ± 0.0011	0.07207	0.0719 ± 0.0011	0.07126	0.07147 ± 0.00091

http://planck.caltech.edu/pub/2013results/Planck_2013_results_16.pdf

Ω_Λ	0.6825	0.686 ± 0.020	0.6964	0.693 ± 0.019	0.6817	$0.685^{+0.018}_{-0.016}$
Ω_m	0.3175	0.314 ± 0.020	0.3036	0.307 ± 0.019	0.3183	$0.315^{+0.016}_{-0.018}$
σ_8	0.8344	0.834 ± 0.027	0.8285	0.823 ± 0.018	0.8347	0.829 ± 0.012
z_{re}	11.35	$11.4^{+4.0}_{-2.8}$	11.45	$10.8^{+3.1}_{-2.5}$	11.37	11.1 ± 1.1
H_0	67.11	67.4 ± 1.4	68.14	67.9 ± 1.5	67.04	67.3 ± 1.2
$10^9 A_s$	2.215	2.23 ± 0.16	2.215	$2.19^{+0.12}_{-0.14}$	2.215	$2.196^{+0.051}_{-0.060}$
$\Omega_m h^2$	0.14300	0.1423 ± 0.0029	0.14094	0.1414 ± 0.0029	0.14305	0.1426 ± 0.0025
$\Omega_m h^3$	0.09597	0.09590 ± 0.00059	0.09603	0.09593 ± 0.00058	0.09591	0.09589 ± 0.00057
Y_P	0.247710	0.24771 ± 0.00014	0.247785	0.24775 ± 0.00014	0.247695	0.24770 ± 0.00012
Age/Gyr	13.819	13.813 ± 0.058	13.784	13.796 ± 0.058	13.8242	13.817 ± 0.048

Ω_Λ		...	Dark energy density divided by the critical density today
t_0		...	Age of the Universe today (in Gyr)
Ω_m		...	Matter density (inc. massive neutrinos) today divided by the critical density
σ_8		...	RMS matter fluctuations today in linear theory
z_{re}		...	Redshift at which Universe is half reionized
H_0	[20,100]	...	Current expansion rate in $\mathrm{km\,s^{-1}Mpc^{-1}}$
$r_{0.002}$		0	Ratio of tensor primordial power to curvature power at $k_0 = 0.002\,\mathrm{Mpc}^{-1}$
$10^9 A_s$		...	$10^9 \times$ dimensionless curvature power spectrum at $k_0 = 0.05\,\mathrm{Mpc}^{-1}$
$\omega_m \equiv \Omega_m h^2$		...	Total matter density today (inc. massive neutrinos)

$\Omega_b h^2$	0.022068	0.02207 ± 0.00033	0.022242	0.02217 ± 0.00033	0.022032	0.02205 ± 0.00028
$\Omega_c h^2$	0.12029	0.1196 ± 0.0031	0.11805	0.1186 ± 0.0031	0.12038	0.1199 ± 0.0027

$\omega_b \equiv \Omega_b h^2$	[0.005, 0.1]	...	Baryon density today
$\omega_c \equiv \Omega_c h^2$	[0.001, 0.99]	...	Cold dark matter density today

Can we find evidence for inflation?

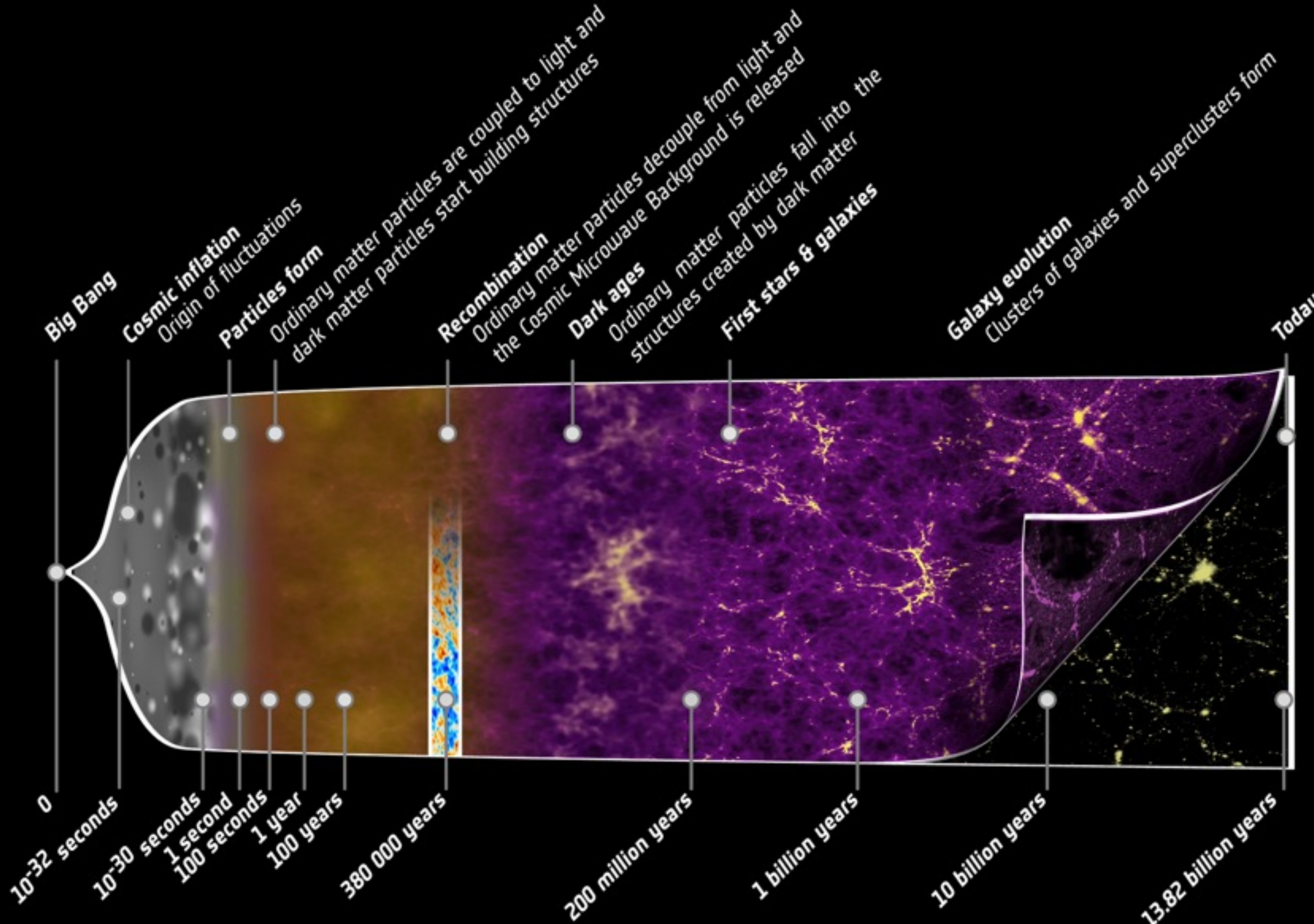

recent excitement turned out to be Fe dust!

Friday Feature™, M. Gold physics 492, Spring 2017